Check for updates

BIOCHEMISTRY

Beyond formic acid: Peptides in carpenter ant venoms aid in disease protection

Lukas Koch[1]†, Sandro Andreotti[2], Mario Schubert[3], Elisa Liebhart[4,5], Anton M. Zürbig[6], Julian Gatzki[7], Benjamin-Florian Hempel[8], Lydia Kollhoff[9,10]‡, Barbara Feldmeyer[11], Martin Herzberg[12], Valerie I. C. Rebhahn[1], Nwet Nwet Win[1], Adria C. LeBoeuf[13], Marat Meleshin[14], Fabian Herrmann[6], Christian Schwieger[7], Heike Brötz-Oesterhelt[4,5], Andrea Sinz[9,10], Mike Schutkowski[14], Timo H. J. Niedermeyer[1]*†§, Simon Tragust[15]*§

Copyright © 2026 The Authors, some rights reserved; exclusive licensee American Association for the Advancement of Science. No claim to original U.S. Government Works. Distributed under a Creative Commons Attribution NonCommercial License 4.0 (CC BY-NC).

Venom peptides are key to the evolutionary success of most venomous animals, including stinging ants. The stingless ant subfamily Formicinae is thought to rely solely on formic acid in their venoms, despite early, unsubstantiated hints of proteinaceous venom constituents. Here, we show that carpenter ants, the largest formicine genus, produce a diverse venom peptide arsenal. Mass spectrometry and transcriptomics across eight geographically distant species uncovered 35 peptides, formicitoxins, belonging to two gene families. Several formicitoxins display antifungal activity. Application to pupae delays fungal outgrowth, suggesting a role of the peptides in colony hygiene. Genome analyses revealed that formicitoxins are widespread but variable across the Formicinae. Our findings overturn the paradigm of formicine venoms as simple acid sprays and establish them as a source of bioactive peptides.

INTRODUCTION

Most ant species (Hymenoptera: Formicidae) are venomous. Following the first isolation of formic acid from *Formica* ants in the dawn of modern chemistry (*1*), it was believed that formic acid served as the principal toxin in the venoms of ants as well as honeybees and other aculeates (*2*). Today, we know that venoms containing concentrated formic acid are an exception and among ants confined to the Formicinae subfamily (*3*). In contrast, venoms composed of peptidic and proteinaceous toxins in aqueous solution are the norm—not only among most ant subfamilies, but across venomous animals in general, including other aculeates such as wasps and bees, chelicerates such as scorpions and spiders, and vertebrates such as snakes and lizards (*4*).

The venoms of the Formicinae subfamily of ants, one of the most speciose and ecologically dominant ant subfamilies, contain formic acid in concentrations ranging from 40% to 70% (*3*). Since the sting is absent in this subfamily, formicine ants expel their venoms through a shared opening of the venom duct and the associated Dufour gland, the so-called acidopore (*3*). Thus, formicine ants may apply their venoms either in close contact by smearing, at a distance by spraying, or directly into wounds inflicted by biting. Beyond their role as biochemical weapons for offense and defense, venoms frequently fulfill additional biological functions (*4*). This is particularly evident in the Formicinae, which spread their venoms onto brood and the surrounding nest environment, using it as an external immune defense trait (*5*, *6*). Moreover, formicine ants have been shown to ingest their venom, thereby acidifying their gut for microbial selection (*7*) (Fig. 1A), and to use it in recruitment signaling and alarm communication (*3*, *4*). It is widely assumed that the primary constituent of these venoms, formic acid, plays a crucial role in this diversity of functions. However, mostly overlooked findings from earlier studies suggest the presence of peptidic compounds in the venoms of formicine ants (*2*, *8*, *9*). Despite their potential involvement in the functions of these venoms, this initial observation has not been investigated to date.

Here, we characterize peptides in the venoms of formicine ants. Combining mass spectrometry and transcriptomics, we identified 35 venom peptides from 13 samples of different carpenter ant (*Camponotus*) species, one of the largest and most diverse ant genera. We describe their structures and bioactivities, discuss their biological functions, mechanism of action, and evolutionary origins, and demonstrate that these peptides belong to two formicitoxin (FRTX) gene families present in at least 21 genera across the Formicinae subfamily. In addition, we present data on the presence of various

[1]Institute of Pharmacy, Freie Universität Berlin, Königin-Luise-Straße 2+4, 14195 Berlin, Germany. [2]Bioinformatics Solution Center, Institute of Computer Science, Freie Universität Berlin, Takustraße 9, 14195 Berlin, Germany. [3]BioSupraMol Core Facility, Freie Universität Berlin, Takustraße 3, 14195 Berlin, Germany. [4]Department of Microbial Bioactive Compounds, Interfaculty Institute of Microbiology and Infection Medicine, University of Tübingen, Auf der Morgenstelle 28, 72076 Tübingen, Germany. [5]Cluster of Excellence "Controlling Microbes to Fight Infection", University of Tübingen, Tübingen, Germany. [6]Institute of Pharmaceutical Biology and Phytochemistry, University of Münster, Corrensstraße 48, 48149 Münster, Germany. [7]Institute of Chemistry, Martin Luther University Halle-Wittenberg, Von-Dankelmann-Platz 4, 06124 Halle (Saale), Germany. [8]Veterinary Centre for Resistance Research, Freie Universität Berlin, Robert-von-Ostertag-Straße 8, 14163 Berlin, Germany. [9]Department of Pharmaceutical Chemistry and Bioanalytics, Institute of Pharmacy, Martin Luther University Halle-Wittenberg, Kurt-Mothes-Straße 3, 06120 Halle (Saale), Germany. [10]Center for Structural Mass Spectrometry, Martin Luther University Halle-Wittenberg, Kurt-Mothes-Straße 3, 06120 Halle (Saale), Germany. [11]Senckenberg Biodiversity and Climate Research Centre (SBiK-F), Georg-Voigt-Straße 14-16, 60325 Frankfurt am Main, Germany. [12]Department of Solar Materials Biotechnology (SOMA), Helmholtz Centre for Environmental Research GmbH (UFZ), Permoserstraße 15, 04318 Leipzig, Germany. [13]Department of Zoology, University of Cambridge, Downing Street, Cambridge CB2 3EJ, UK. [14]Department of Enzymology, Institute of Biochemistry and Biotechnology, Martin Luther University Halle-Wittenberg, Kurt-Mothes-Straße 3a, 06120 Halle (Saale), Germany. [15]Department of General Zoology, Institute of Biology, Martin Luther University Halle-Wittenberg, Hoher Weg 8, 06120 Halle (Saale), Germany.
*Corresponding author. Email: timo.niedermeyer@fu-berlin.de (T.H.J.N.); simon.tragust@zoologie.uni-halle.de (S.T.)
†Part of this work was conducted at the Department of Pharmaceutical Biology/Pharmacognosy, Institute of Pharmacy, Martin Luther University Halle-Wittenberg, Hoher Weg 8, 06120 Halle (Saale), Germany.
‡Present address: Section Clinical Mass Spectrometry, Institute of Laboratory Medicine, Clinical Chemistry, and Molecular Diagnostics, Leipzig University Medical Center, Liebigstraße 27a, 04103 Leipzig, Germany.
§These authors contributed equally to this work.

Downloaded from https://www.science.org at Cambridge University on July 16, 2026

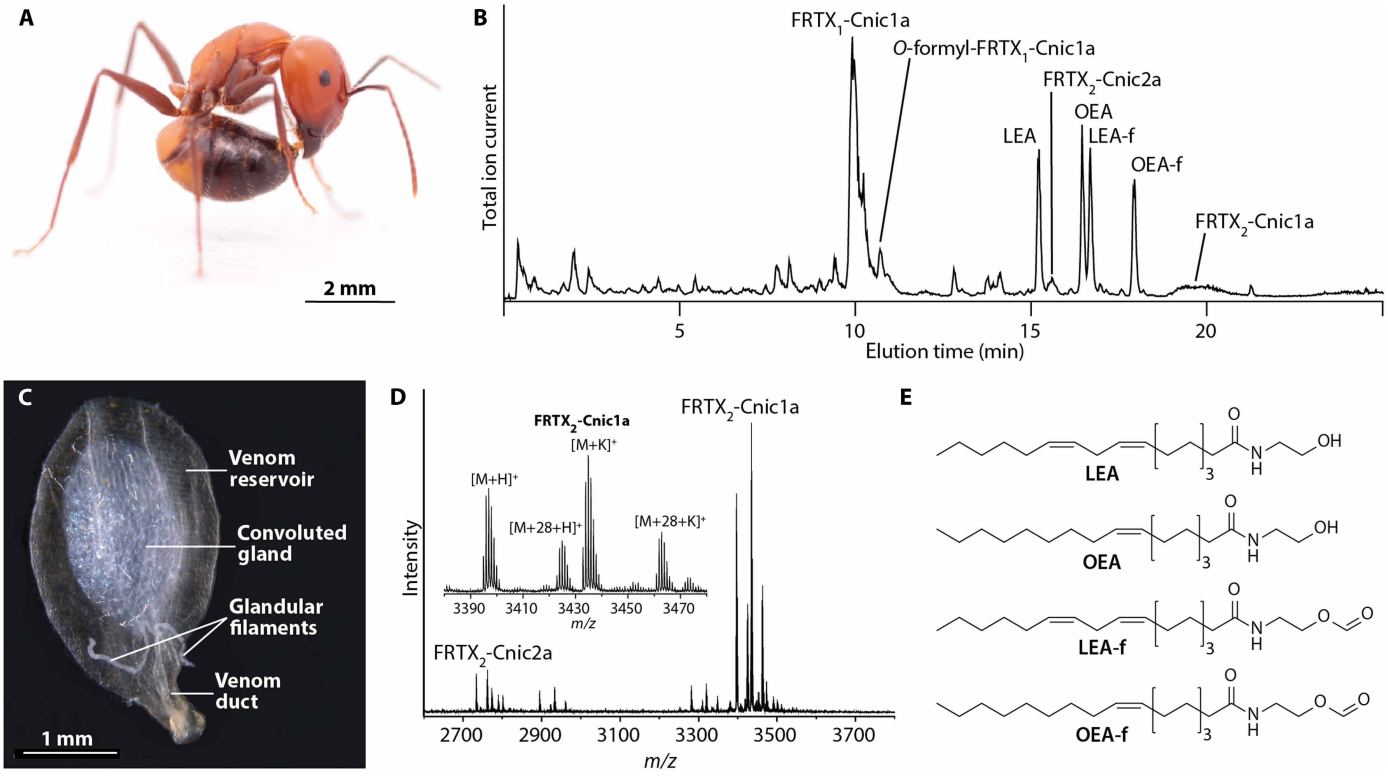


Fig. 1. Analysis of *C. nicobarensis* venom. (**A**) *C. nicobarensis* major worker during acidopore grooming. (**B**) Total ion current chromatogram of *C. nicobarensis* venom. Major peaks corresponding to venom peptides are labeled as formicitoxins $FRTX_1$-Cnic1a (LDIKEIINKIISDIKEKIAKAL), $FRTX_2$-Cnic1a (DIVSFLLELPKIIEEFFLKLINLFKLIF), and $FRTX_2$-Cnic2a (NILSNIIDSIIHLLFEDFSRIFL). Signals corresponding to *N*-acylethanolamines (NAEs) are labeled as linoleoyl ethanolamide (LEA), oleoyl ethanolamide (OEA), linoleamidoethyl formate (LEA-f), and oleamidoethyl formate (OEA-f). (**C**) Dissected venom apparatus of a *C. nicobarensis* major worker as used for extraction of venom and RNA. (**D**) MALDI mass spectrum of *C. nicobarensis* venom showing molecular ions of $FRTX_2$-Cnic1a and $FRTX_2$-Cnic2a along with potassium adducts (+39 Da) and formyl esters (+28 Da). Inset: Magnified mass/charge ratio (*m*/*z*) range 3350 to 3550. (**E**) Structures of LEA, OEA, LEA-f, and OEA-f.

lipids in the venoms of carpenter ants, illustrating that carpenter ant venoms are far more complex than previously recognized.

RESULTS AND DISCUSSION

The venom of *Camponotus nicobarensis* contains peptides and lipids

To test our hypothesis that formicine ant venoms contain peptides, we analyzed the venom of *Camponotus nicobarensis* workers using electrospray ionization tandem mass spectrometry coupled to high-performance liquid chromatography (HPLC-ESI-MS/MS). We found the total ion current chromatogram of *C. nicobarensis* venom dominated by a major peak corresponding to a compound with a monoisotopic mass of 2507.5300 Da (Fig. 1B). Next, we sequenced the venom apparatus transcriptome of *C. nicobarensis* and applied a proteotranscriptomic workflow consisting of MS-based de novo peptide sequencing combined with a BLAST search against the transcriptome to identify the compound as a docosapeptide we named formicitoxin $FRTX_1$-Cnic1a. Two additional peptides, $FRTX_2$-Cnic1a and $FRTX_2$-Cnic2a, were identified from lower-intensity signals (for nomenclature, see Supplementary Text). To the best of our knowledge, these compounds are the first peptides from the venom of a formicine ant species that have been identified to amino acid sequence level. No matches resulted from BLAST queries against the National Center for Biotechnology Information (NCBI) core nucleotide and whole-genome shotgun contig sequence databases. Despite sharing little sequence similarity, all three peptides were predicted to adopt amphipathic α-helical conformations in solution (data S1)—a common property among venom peptides with antimicrobial activity (*10*, *11*). Each peptide was found accompanied by smaller amounts of derivatives that were truncated or deamidated on glutamine or asparagine residues. We also detected *O*-formylated variants of the peptides, as evidenced by a mass increase of 28 Da at serine residues and a neutral loss of 46 Da, consistent with the elimination of formic acid. The observed truncation, deamidation, and formylation of the peptides can well be explained by prolonged exposure to concentrated formic acid (*12*, *13*), implying that these compounds are produced and stored in the venom reservoir (Fig. 1C). This was confirmed by HPLC-ESI-MS/MS analysis of the content of a dissected reservoir, which was found to be identical to the venom expelled by the ants upon mechanical stimulation.

Next, we analyzed the venom of *C. nicobarensis* using matrix-assisted laser desorption/ionization mass spectrometry (MALDI-MS). While $FRTX_1$-Cnic1a could not be detected, $FRTX_2$-Cnic1a and $FRTX_2$-Cnic2a were observed, along with smaller amounts of truncated and formylated derivatives (Fig. 1D). However, both peptides were predominantly detected as their potassium adducts in MALDI-MS. This prompted us to analyze the metal contents of the venom using inductively coupled plasma mass spectrometry (ICP-MS). Potassium was found to be indeed the most abundant metal

Downloaded from https://www.science.org at Cambridge University on July 16, 2026

ion in the venom (1.3 mg ml^{-1}), along with smaller amounts of iron and calcium (table S1), consistent with early reports on the composition of formicine ant venoms (*3*). While alkali metal adducts are commonly observed in MALDI-MS of ant venom peptides (*14*), little is known on the concentrations and functions of metal ions in ant venoms. However, the prevenom of the scorpion *Parabuthus transvaalicus* has been shown to contain elevated concentrations of potassium (3.2 mg ml^{-1}), aiding in the paralysis of prey (*15*).

In addition to the peptides, we identified two known *N*-acylethanolamines (NAEs), oleoyl ethanolamide (OEA) and linoleoyl ethanolamide (LEA), in the venom of *C. nicobarensis* (Fig. 1E, fig. S1, and Supplementary Text). While these compounds are known signaling lipids in animals (*16*), they have, to the best of our knowledge, not yet been reported as constituents of an animal venom. Both LEA and OEA are known to influence the growth of different bacteria (*17*), possibly assisting a function of the venom in microbial control. As for the FRTX peptides, OEA and LEA were accompanied by their formyl esters LEA-f and OEA-f. We hypothesized that LEA-f and OEA-f form spontaneously from LEA and OEA in the presence of concentrated formic acid. Overnight incubation of synthetic OEA and LEA in neat formic acid procured complete conversion to their formic acid esters, which are identical to the compounds found in the venom as judged by HPLC-ESI-MS/MS (figs. S2 to S9). Repeating this reaction on a preparative scale allowed us to confirm the structures of LEA-f and OEA-f using nuclear magnetic resonance (NMR) spectroscopy (figs. S11 to S18). While formylation of peptides and proteins exposed to formic acid is well-known (*12*), we are not aware of any application of this reaction in the synthesis of formic acid esters, which usually requires catalysts or activating agents. Of note, the free NAEs and their formic acid esters exist in equilibrium, and the ratios of LEA to LEA-f and OEA to OEA-f provide a convenient estimate of the formic acid concentration in *Camponotus* venoms (table S2 and Supplementary Text). Further analysis of the HPLC-MS/MS data revealed the presence of lysophosphatidyl cholines (LPC 18:1, 18:2, and 20:1) in the venom, which were not characterized in further detail (fig. S10). LPCs are also present in the venom of the predatory waterbug *Belostoma anurum*, where they contribute to prey paralysis (*18*).

Formicitoxins are widespread among carpenter ants and across the Formicinae subfamily

Having discovered three peptides in the venom of *C. nicobarensis*, we set out to explore the diversity of venom peptides across the *Camponotus* genus. Thus, we extended our proteotranscriptomic workflow to samples from 13 ant colonies representing eight species and species complexes, originating from Europe, Africa, North America, and Asia (Fig. 2A and fig. S19). For each colony, we analyzed venom samples using HPLC-ESI-MS/MS and sequenced transcriptomes of venom apparatuses and residual body tissues. Searching de novo peptide sequences deduced from HPLC-ESI-MS/MS datasets against the transcriptomes, we identified a total of 35 formicitoxin peptides from the venoms of *C. fallax*, *C. fellah*, *C.* cf. *floridanus*, *C. japonicus*, *C. ligniperda*, *C.* cf. *maculatus*, *C. nicobarensis*, and *C. vicinus* (Fig. 2C). All samples contained the NAE and LPC lipids also found in the venom of *C. nicobarensis*. In addition, using bottom-up proteomics, we detected phospholipase B–like proteins in all 13 and icarapin-like proteins in 11 samples (data S2). While phospholipase B likely accounts for the presence of LPCs detected in *Camponotus* venoms, the function of icarapin-like proteins is unknown. However, icarapin is a major allergen of honeybee venom, from which it was originally discovered (*19*).

A maximum likelihood tree of all identified open reading frames (ORFs) coding for FRTX peptides revealed that all *Camponotus* formicitoxins can be grouped into two gene families, $FRTX_1$ and $FRTX_2$, each characterized by the highly conserved prepropeptide region (Fig. 2C, fig. S20, and data S3 and S4). Using the prepropeptide regions in $FRTX_1$ and $FRTX_2$ coding sequences as bioinformatic handles, we identified 155 formicitoxins from 62 formicine ant species (data S6), covering 21 formicine ant genera (data S7 and S8). This set includes close analogs of the peptides detected using proteotranscriptomics such as $FRTX_1$-Cfel1b and $FRTX_1$-Cvic1b, as well as re-identified $FRTX_1$-Cjap1a, $FRTX_1$-Cflo1b, $FRTX_1$-Cfel1a, $FRTX_2$-Cflo1a, and $FRTX_2$-Cvic4a (figs. S21 and S22).

Focusing on the evolutionary origins of the formicitoxins, we conducted BLAST and Exonerate searches against a total of 112 ant and non-ant hymenopteran genomes. The results indicate the presence of FRTX peptides in the Formicinae subfamily only. We found zero to eight copies of each gene per species, often localized in the same scaffold or chromosome (data S9 and S10). This observation matches the organization of venom peptides in tandem repeats in the genome of the stinging ant *Tetramorium bicarinatum* (*20*). We further constructed a maximum likelihood phylogeny of the formicitoxins and representatives of all known hymenopteran venom gene families, in which FRTX peptides form a separate branch with two clades corresponding to $FRTX_1$ and $FRTX_2$ peptides, respectively (data S11). Moreover, we tested the sequences for conserved domains using HMMER but did not detect any known domains (data S12 and S13). Together, these results indicate that the formicitoxins evolved in the Formicinae lineage. However, more in-depth comparative genomic analyses would be needed to resolve the evolutionary history of aculeate venom peptide families (*21*).

Camponotus formicitoxins are subject to qualitative and quantitative variation

Generally, we found that each *Camponotus* species is armed with its own arsenal of two to five venom peptides from both formicitoxin families (Fig. 2C, figs. S23 to S39, and table S3). However, we found considerable variation between samples within the *C. floridanus*/*atriceps* and *C. maculatus* species complexes. For instance, $FRTX_2$-Cflo1a and $FRTX_2$-Cflo2a are found in all three samples from the *C. floridanus*/*atriceps* species complex, while $FRTX_1$-Cflo1a is only found in sample CFLO1 and replaced by $FRTX_1$-Cflo2a and $FRTX_1$-Cflo2b in samples CFLO2 and CFLO3. Whether this diversity is due to intraspecific variation, i.e., caused by allelic diversity as has been described for *Rhytidoponera metallica* (*22*), or rather interspecific variation between cryptic species as was observed for ponerine ants (*14*), remains to be established. In contrast, invariably the same peptides were detected in the venoms of five *C. ligniperda* colonies sampled from distant geographical locations in Germany, Switzerland, and Italy, albeit in differing relative quantities (figs. S29 to S33 and S40).

Using a synthetic standard, we quantified $FRTX_1$-Cnic1a in venom samples of *C. nicobarensis* and found a mean concentration of 0.36 ± 0.05 mg ml^{-1} (fig. S41). For five additional formicitoxins in the venoms of *C. nicobarensis* and *C. floridanus*, we estimated concentrations between 0.02 and 0.28 mg ml^{-1}, the variation in concentrations between different peptides being greater than between concentrations of the same peptide in different venom samples

Downloaded from https://www.science.org at Cambridge University on July 16, 2026

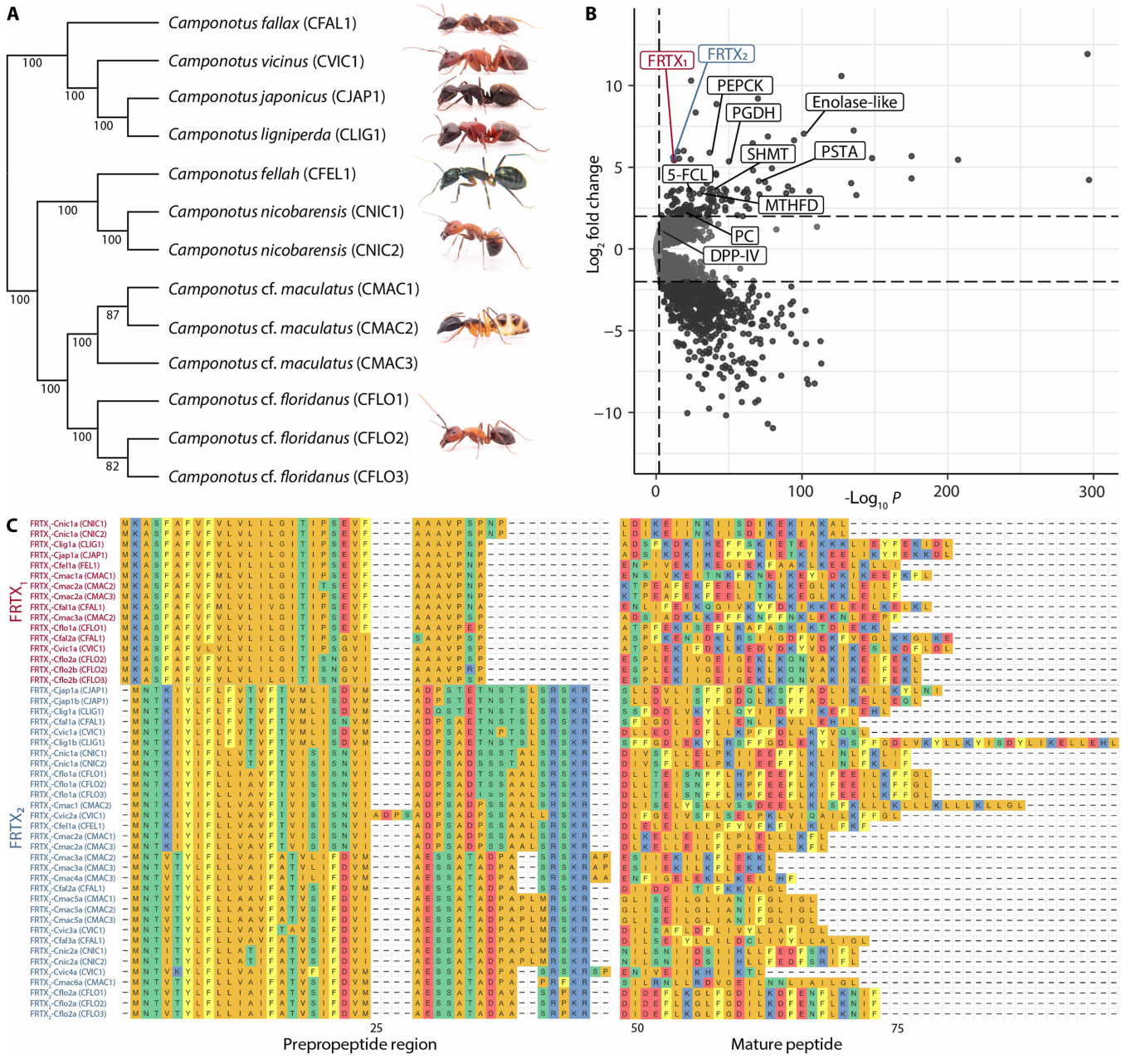


Fig. 2. Proteotranscriptomic analysis of *Camponotus* venoms. (**A**) Cladogram, species names, and representative photographs of ants used in this work. The phylogenetic relationships between ant samples were reconstructed by mapping raw RNA sequencing reads to 100 reference genes using read2tree. Bootstrap values were calculated from 1000 replicates. Species identities were confirmed using DNA barcoding of the cytochrome oxidase subunit I gene. (**B**) Volcano plot representing differential gene expression of venom apparatus versus residual body tissues across all *Camponotus* samples. Cutoffs were 0.01 for *P* and 2 for $\log_2$-fold change, respectively. Formicitoxins: $FRTX_1$, formicitoxin family I–type peptides; $FRTX_2$, formicitoxin family II–type peptides; DPP-IV, venom dipeptidyl peptidase IV; enzymes involved in formic acid biosynthesis: 5-FCL, 5-formyl tetrahydrofolate cycloligase; MTHFD, methylenetetrahydrofolate dehydrogenase/cyclohydrolase; PC, pyruvate carboxylase; PEPCK, phosphoenol pyruvate carboxykinase; PGDH, 3-phosphoglycerate dehydrogenase; PSTA, phosphoserine transaminase. (**C**) Multiple sequence alignment of FRTX-coding ORFs identified by mass spectrometry and mRNA sequencing. Nucleotide sequences of the prepropeptide region (1–47) were codon-aligned using MUSCLE and translated. A gap was introduced in position 48 to separate preprosequences and mature peptides as determined by mass spectrometry (not aligned). Colony sample names are given in parentheses. In sample CFLO3, $FRTX_1$-Cflo2a was detected with mass spectrometry but not in the transcriptome. Amino acid color scheme: orange, aliphatic; yellow, benzylic; green, hydrophilic; blue, basic; red, acidic. Photo credit (photograph of *C. fellah*): Z. Zhao, University of Cambridge.

Downloaded from https://www.science.org at Cambridge University on July 16, 2026

(table S4). These concentrations are somewhat lower than the concentrations of ponericin peptides found in the venom of the similar-sized stinging ant *Neoponera goeldii* (1 to 46 mg ml^{-1}) (*23*). However, large *Camponotus* workers can store up to 6 µl of venom in their venom reservoirs (*3*, *24*), and in our hands, workers of *C. nicobarensis* and *C. floridanus* frequently ejected volumes larger than 1 µl, exceeding the total venom reservoir volume of *N. goeldii* (0.17 µl) by a factor of 5 to 10. Thus, the total amount of a peptide delivered in a single venom dose may be comparable.

Camponotus formicitoxins and genes for formic acid biosynthesis are differentially expressed in venom gland tissues

A differential gene expression (DGE) analysis comparing expression levels in dissected venom apparatuses versus residual body tissue (carcasses) revealed that FRTX-coding genes are differentially expressed in venom apparatus tissues ($FRTX_1$: 42-fold higher expression, $FRTX_2$: 49-fold higher expression; Fig. 2B, figs. S42 and S43, and data S14). While this finding confirms that the formicitoxins are venom peptides sensu stricto and not ubiquitous compounds unintentionally secreted into the venom, FRTX-coding transcripts were also detected in the residual body tissues. This may be explained by either contamination with venom apparatus tissue or transcription of these genes in other body parts, e.g., the fat body, as was recently described for the honeybee venom peptide melittin in response to bacterial infection (*25*). In addition to FRTX-coding genes, phospholipase B and icarapin genes are up-regulated in the venom apparatus. Further, we found genes coding for enzymes involved in one-carbon metabolism and serine biosynthesis to be differentially expressed in venom apparatus tissues (100-fold to 132-fold), bolstering the proposed biosynthetic pathway for formic acid in formicine ants from serine via tetrahydrofolate-bound one-carbon intermediates (*3*, *26*, *27*). Notably, the up-regulation of phosphoenol pyruvate carboxykinase (PEPCK) may enable funneling of tricarboxylic acid cycle-derived carbon atoms to serine biosynthesis. This would render formic acid biosynthesis independent from dietary uptake of serine, which might be of crucial advantage under conditions of protein scarcity.

Formicitoxins are translated as prepropeptides and processed by at least two venom peptidases

The ORFs coding for formicitoxins encode longer peptides than those detected in the venoms, suggesting that formicitoxins are translated as precursor peptides (Fig. 2C). The N-terminal regions of these prepropeptides are predicted to contain signal sequences, which direct co-translational transport by the Sec translocon and are subsequently cleaved by signal peptidase I (SPI; data S15). Within the $FRTX_1$ gene family, the resulting propeptides exhibit a repeating pattern where every second amino acid up to the secreted peptide is either proline or alanine. Such propeptides are thought to undergo stepwise cleavage by dipeptidyl peptidase IV (DPP-IV)–like proteases, a process that has been well characterized for the principal toxin of honeybee venom, melittin (*28*). We frequently detected small amounts of unprocessed or partially processed propeptides of the $FRTX_1$ family in *Camponotus* venoms that were consistent with sequential cleavage of dipeptides (figs. S23, S28 to S33, and S40), and genes coding for venom dipeptidyl peptidase IV–like proteins were found to be up-regulated in the venom apparatuses (Fig. 2B). Like $FRTX_1$ propeptides, $FRTX_2$ propeptides contain dipeptide repeats where every second amino acid residue is alanine or proline. In addition, $FRTX_2$ propeptides contain a highly conserved RXKR motif, suggesting that $FRTX_2$ peptides are eventually liberated by a basic amino acid–specific proprotein convertase (PPC) (*29*). In most cases, this cleavage site directly precedes the sequence of the mature venom peptides, except for $FRTX_2$-Cmac3a, 4a, and 6a, where an additional DPP-IV–cleavable dipeptide follows the PPC cleavage site. DPP-IV–cleavable propeptides are also known from the aculeatoxins, a proposed hyperdiverse gene superfamily comprising venom peptides from stinging ants, wasps, and bees (*20*). It is, however, interesting to note that FRTX propeptides, in contrast to aculeatoxin propeptides, are generally not acidic. PPC-mediated processing of venom peptides is common in animals but uncommon in aculeate hymenopterans, where PPC-independent SPI/DPP-IV processing is the norm (*30*).

Formicitoxins are antifungal peptides that can protect brood from fungal infection

Venom peptides from stinging ants and other arthropods are known to exhibit potent algogenic, cytotoxic, insecticidal, paralyzing, or antimicrobial activities that make them effective tools to deter predators, subdue prey, and ward off microbial infections (*11*, *23*, *31*–*39*). To explore the bioactivities and potential functions of the formicitoxins, we synthesized seven representatives ($FRTX_1$-Cfel1a, $FRTX_1$-Cflo1a, $FRTX_2$-Cfel1a, $FRTX_1$-Cnic1a, $FRTX_2$-Cflo1a, $FRTX_2$-Cnic1a, and $FRTX_2$-Cnic2a), selected to cover both gene families $FRTX_1$ and $FRTX_2$ and most peptides from the venoms of *C. nicobarensis*, *C. fellah*, and *C.* cf. *floridanus*, and subjected them to assays for insecticidal and antimicrobial activity.

Like stinging ants, formicine ants use their venoms in predation (*3*). However, when injected into blowfly (*Lucilia caesar*) larvae as a prey model, none of the tested FRTX peptides produced notable paralyzing or lethal effects (fig. S53). This lack of activity is perhaps unsurprising, as the high concentrations of caustic and cytotoxic formic acid in formicine ant venoms likely alleviate the need for additional paralyzing or insecticidal peptide toxins. In addition, formicine ants are not armed with stings and thus do not have an efficient delivery mechanism for compounds that cannot penetrate the cuticles of arthropod prey, although spraying venom into bite wounds may provide an alternative (*3*).

Next to their most evident role in predation and defense against competitors, hymenopteran venom peptides have also been proposed to contribute to the immune defense of their producers (*10*, *11*), suggesting a dual function of these venoms as weapons and disinfectants. In support of this, antimicrobial venom substances have been detected on nesting materials and body surfaces of bees, wasps, and ants (*40*–*44*), and the sanitary use of venom secretions is well documented in formicine ants (*3*). Formicine ants of various genera have been observed applying their venom onto fungus-infected brood as a means of disinfection (*45*–*47*), occasionally even sacrificing brood to contain pathogen spread within the nest (*48*). Since the formicitoxins are predicted to adopt amphipathic α-helical structures (data S1), a characteristic of antimicrobial peptides (AMPs), we tested synthetic formicitoxins for antimicrobial activity.

The peptides showed negligible antibacterial effects against *Serratia marcescens*, *Bacillus subtilis*, *Enterococcus faecalis*, and *Pseudomonas aeruginosa*, with the most pronounced but still weak inhibition observed for *B. subtilis* by $FRTX_1$-Cflo1a (figs. S54 to S57).

The peptides subsequently were tested against entomopathogenic and opportunistic fungi. Four of the seven tested formicitoxins

Downloaded from https://www.science.org at Cambridge University on July 16, 2026

showed concentration-dependent antifungal activity against the opportunistic entomopathogens *Metarhizium pingshaense* and *Beauveria bassiana* as well as a *Penicillium brocae* strain isolated from a *C. nicobarensis* pupa (Fig. 3, A to C, and fig. S58). Two peptides, $FRTX_1$-Cnic1a and $FRTX_2$-Cflo1a, exhibited potent to moderate inhibitory effects against all three fungal isolates [median inhibitory concentration (IC_{50}) between 0.5 and 2.2 μM]. Their antifungal activity exceeded that of the human AMP LL-37 against *P. brocae* and *M. pingshaense* (IC_{50} > 8 μM). Against *P. brocae*, they achieved lower molar IC_{50} values than the antifungal drug substance voriconazole (0.9 μM and 0.5 μM versus 2.0 μM). In contrast, $FRTX_1$-Cflo1a displayed only weak activity against all three fungal isolates. $FRTX_1$-Cfel1a was only weakly active against *B. bassiana* and *M. pingshaense* (IC_{50} 1.9 μM and 1.5 μM but only 35% and 40% maximal inhibition) while showing stronger inhibition of *P. brocae* (IC_{50} 1.6 μM, >70% inhibition), suggesting that the antifungal activity of the formicitoxins is at least partially strain-specific. Accordingly, the high degree of sequence variation among formicitoxins from different carpenter ant species may reflect selection pressures imposed by habitat-specific fungal pathogens.

Motivated by the antifungal activity of the formicitoxins in the in vitro experiments, we decided to investigate if this activity would increase the survival of fungus-infected ant pupae. Using an optical pH sensor, we first confirmed that *C. nicobarensis* pupae display strong surface acidity that declines when pupae are removed from the colony (fig. S59). This suggests that *C. nicobarensis* workers apply their acidic venom onto brood, which is in line with earlier observations that formicine ants routinely deploy venom around their nesting environment (*49*). Next, we treated pupae with $FRTX_1$-Cnic1a (240 ng or 96 pmol per pupa, equivalent to ~700 nl of venom) and *M. pingshaense* conidiospores, and monitored fungal outgrowth in the presence of workers (Fig. 3D and fig. S60). Although all pupae eventually succumbed to the high dose of conidiospores used in the experiment, fungal outgrowth was significantly delayed on pupae treated with $FRTX_1$-Cnic1a ($P = 0.003$, hazard ratio: 1.571). The same effect was found when the experiment was repeated in the absence of workers ($P = 0.004$, hazard ratio: 1.514). Together, these experiments suggest that the antifungal activity of $FRTX_1$-Cnic1a can protect pupae from fungal infection when the acute antimicrobial effects of formic acid wear off due to evaporation.

Downloaded from https://www.science.org at Cambridge University on July 16, 2026

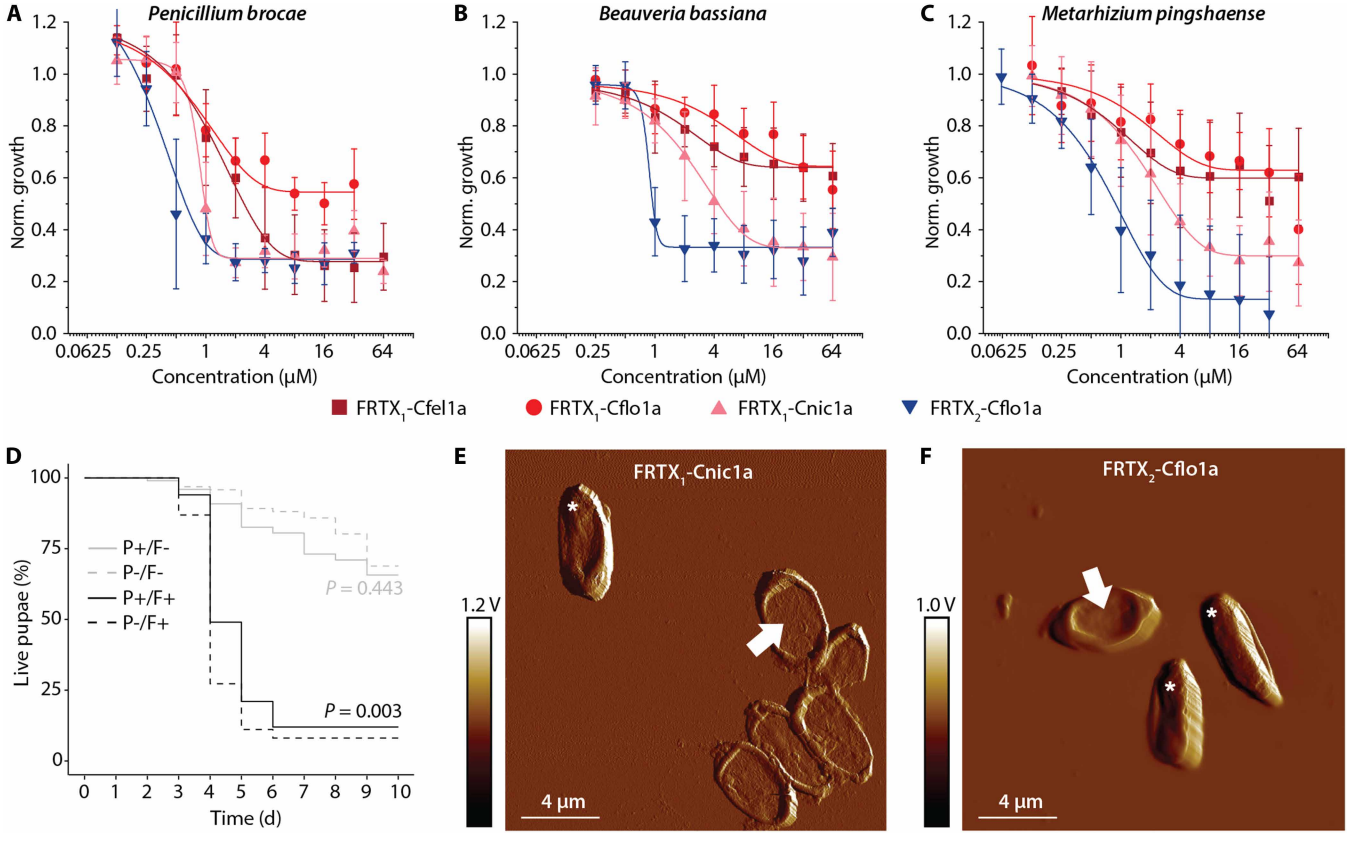


Fig. 3. Antifungal activity of formicitoxins. (**A** to **C**) Growth inhibition (growth normalized to growth control) of *P. brocae*, *B. bassiana*, and *M. pingshaense* in the presence of $FRTX_1$-Cfel1a, $FRTX_1$-Cflo1a, $FRTX_1$-Cnic1a, and $FRTX_2$-Cflo1a (WST-8–based microtiter plate assay). (**D**) Survival of *C. nicobarensis* pupae treated with conidia of the entomopathogenic fungus *M. pingshaense* (F) and the peptide $FRTX_1$-Cnic1a (P) or controls. Pupae were kept in groups of four, each with two workers. Each treatment group contained $N = 100$ pupae. Treatments P+/F− and P+/F+ were compared with treatments P−/F− and P−/F+, respectively (P+/F− versus P−/F−: COXME: LR-test, $\chi^2 = 0.589$, df = 1, $P = 0.443$; P+/F+ versus P−/F+: Cox Mixed Effects Model (COXME): Likelihood Ratio (LR)-test, $\chi^2 = 8.8792$, df = 1, $P = 0.003$, hazard ratio: 1.571). (**E** and **F**) Ultrastructural images of *M. pingshaense* conidia treated with $FRTX_1$-Cnic1a or $FRTX_2$-Cflo1a (atomic force microscopy). Characteristic defects are highlighted with arrows. Conidia without visible defects are marked with an asterisk.

Formicitoxins are amphipathic peptides that target biological membranes

Despite variation in length and sequence, as discussed above, all identified FRTX peptides are predicted to adopt amphipathic α-helical conformations (data S1) characteristic for AMPs that target biological membranes (*50*). Principal components analysis revealed that peptides from each FRTX gene family occupy a confined section of physicochemical space defined by molecular weight, net charge, isoelectric point, and hydrophobicity (fig. S61A and data S16 and S17). This conservation of physicochemical properties rather than sequence motifs further suggests that formicitoxins may target biological membranes rather than specific proteins, and that each formicitoxin family may have different mechanisms of action. Generally, $FRTX_1$ peptides have isoelectric points >6.0 and are only moderately hydrophobic, whereas most $FRTX_2$ peptides have isoelectric points <6.0 and are more hydrophobic (fig. S61B). In contrast, most known AMPs are polycationic, which is also true for AMPs from ant venoms (*39*), although anionic AMPs are known (*51*–*53*). Since many AMPs also display hemolytic activity caused by interaction with the membrane bilayers of erythrocytes, we subjected our synthetic formicitoxins to hemolytic activity assays.

Three of the seven tested formicitoxins displayed concentration and pH-dependent hemolytic activity against sheep erythrocytes in low micromolar concentrations (fig. S62), confirming that these peptides are membranolytic. Unlike the antifungal effects, which we found for peptides from both formicitoxin subfamilies $FRTX_1$ and $FRTX_2$, hemolytic activity was exclusively found within the $FRTX_2$ family ($FRTX_2$-Cnic2a, -Cflo1a, and -Cfel1a).

On the basis of their antifungal activity, we selected $FRTX_1$-Cnic1a and $FRTX_2$-Cflo1a for more detailed structural and mechanistic investigations. First, we examined whether exposure of fungal spores to these peptides would induce morphological changes. Using phase-contrast microscopy and atomic force microscopy (AFM), we observed that *M. pingshaense* conidia treated with $FRTX_1$-Cnic1a and $FRTX_2$-Cflo1a exhibit characteristic defects (Fig. 3, E and F, and figs. S63 to S65). Upon treatment with $FRTX_1$-Cnic1a in phosphate-buffered saline, conidiospores and germination tubes appear flattened and fragmented. Exposure to $FRTX_2$-Cflo1a led to granulation and flattening of the central area of the spores, resulting in a donut-like appearance. These defects can be interpreted as signs of plasma loss as it would result from permeabilization of the plasma membrane. On the other hand, peptide-treated conidia were not stained when exposed to propidium iodide, suggesting that the plasma membranes remain at least partially intact (figs. S66 and S67). Membrane-disrupting peptides have also been described from stinging ant venoms (*54*, *55*).

Next, to confirm the predicted α-helical structures of these peptides, we decided to perform solution NMR experiments of synthetic $FRTX_1$-Cnic1a and $FRTX_2$-Cflo1a (see Supplementary Text). The ^1H NMR spectrum of $FRTX_1$-Cnic1a in aqueous solution indicated formation of aggregates, leading to line broadening and poor dispersion (fig. S68A). In a mixture of 2,2,2-trifluoroethanol (TFE) and water, $FRTX_1$-Cnic1a adopted the predicted α-helical structure as judged by two-dimensional heteronuclear single-quantum coherence (HSQC) and nuclear Overhauser effect spectroscopy (NOESY) NMR experiments (figs. S68B, S69, S71, S73, and S75). Similarly, $FRTX_2$-Cflo1a adopted a mostly α-helical conformation in TFE/water (figs. S68C, S70, S72, S74, and S76), while its structure in aqueous solution could not be determined due to its low solubility. Many expected through-space nuclear Overhauser effect correlations were missing in the region preceding Pro^{13} of $FRTX_2$-Cflo1a, indicating a kinked helix as predicted by PepFold and AlphaFold3 (fig. S77). These predicted structures show that the hydrophobic face of the helix is located on the inner side of the angle. Thus, integration into a planar membrane would either require partial unwinding of the helix or result in disturbance and bending of the membrane. Under the conditions of our measurements, the His^{12}-Pro^{13} peptide bond was found to be in trans configuration based on a C^{β}-C^{γ} chemical shift difference of 2.9 parts per million (ppm) (*56*). Of note, most of the 13 venoms analyzed in this work contain an $FRTX_2$ peptide with a central proline residue, corroborating its functional importance.

To gain further insight into the interaction of both peptides with biological membranes, we next studied their insertion into model lipid monolayers by measuring changes of the surface pressure after injection of the peptides into the aqueous subphase (fig. S78). Both $FRTX_1$-Cnic1a and $FRTX_2$-Cflo1a showed maximum insertion pressures (MIPs) greater than the monolayer-bilayer equivalence pressure of 30 mN m^{-1} in 1-palmitoyl-2-oleoyl-*sn*-glycero-3-phosphocholine (POPC) monolayers (*57*, *58*). The MIP of $FRTX_2$-Cflo1a was found to be much higher than that of $FRTX_1$-Cnic1a (47 versus 35 mN m^{-1}) and comparable to that of honeybee melittin (45 mN m^{-1}), which is well-known to bind to and disrupt biomembranes (*59*, *60*). These results are consistent with the hemolytic activity of both melittin and $FRTX_2$-Cflo1a, which is lacking for $FRTX_1$-Cnic1a (*61*). Finally, we used infrared reflection absorption spectroscopy (IRRAS) and film balance measurements to probe the kinetics and orientation of the adsorption of the peptides to POPC monolayers (fig. S79, A and C). Judging from pressure isotherms and amide I integrals, $FRTX_1$-Cnic1a inserted into the monolayer within minutes, whereas $FRTX_2$-Cflo1a insertion required several hours to complete (fig. S79, B and D). Despite its slower binding kinetics, $FRTX_2$-Cflo1a exhibited more extensive binding to the monolayer, as evidenced by a higher amide I band integral after complete adsorption [60 milli Reflectance-Absorbance (mRA) cm^{-1} versus 30 mRA cm^{-1} for $FRTX_1$-Cnic1a], consistent with its higher MIP. The amide I band positions ($FRTX_1$-Cnic1a: 1658 cm^{-1}, $FRTX_2$-Cflo1a: 1661 cm^{-1}) confirm that both peptides adopt an α-helical structure upon binding to the monolayer, in agreement with our structure predictions and solution NMR data. Global fitting of the angle-dependent IRRA spectra yielded a helix tilt angle of $\theta = 90°$ with respect to the monolayer layer normal for both peptides, equivalent to a parallel orientation with respect to the lipid surface.

In conclusion, we identified and characterized the formicitoxins—the first venom peptides reported from the Formicinae, one of the most species-rich ant subfamilies. Previously considered to be simple formic acid sprays, carpenter ant venoms are now shown to be complex mixtures of formic acid, peptides, proteins, and lipids. Furthermore, we demonstrate that formicitoxin-coding genes are present across multiple genera within the Formicinae subfamily and display considerable diversity within genera and even closely related species, revealing a vast source of previously overlooked bioactive peptides. Several formicitoxins exhibit activity against entomopathogenic fungi. Given that formicine ants deploy their venoms onto nesting materials and brood, we propose that the role of the formicitoxins is to reinforce this external immune defense: While concentrated formic acid has strong immediate antimicrobial effects, the formicitoxins may serve as a persistent antifungal protective cloak after formic acid has lost its potency due to evaporation, dilution, or

Downloaded from https://www.science.org at Cambridge University on July 16, 2026

neutralization. However, we only determined the activity of selected formicitoxins against selected model organisms, and therefore cannot conclude on broader ecological implications, e.g., to which extent the formicitoxins help shape nest microbiomes. Conversely, we are ignorant of how formicine ants, in turn, alter their venom composition in response to changes in their environment, e.g., microbial challenges. Although inactive when injected into blowfly larvae, we cannot rule out that FRTX peptides may exhibit insecticidal activity against other arthropods, most notably other ants. In addition, future work should investigate possible synergistic actions with other venom components such as formic acid and lipids. The formicitoxins can be clearly delineated into two gene families, unique to the Formicinae subfamily. The peptides from these gene families differ in their physicochemical properties, hemolytic activity, and at least in case of $FRTX_1$-Cnic1a and $FRTX_2$-Cflo1a in membrane MIP and effects on the morphology of fungal spores, suggesting distinct functions and mechanisms of action. Future work should address in more detail the mechanisms by which these molecular properties translate into biological function. Given that formicine ants are dominant in various ecosystems and, as eusocial insects, reliant on effective infection control, the formicitoxins offer a compelling model to investigate how lifestyle and environmental pressures drive the evolution of venom as a key adaptive trait.

MATERIALS AND METHODS

Camponotus workers were collected in the wild or from lab-reared colonies. Ant species were determined morphologically and by cytochrome oxidase subunit I DNA barcoding. Phylogenetic relationships between *Camponotus* samples were inferred by mapping raw RNA-sequencing (RNA-seq) reads against 100 hymenopteran reference genes using read2tree (*62*). Venoms were expelled by workers upon mechanical stimulation, collected with glass capillaries, pooled, and stored at −70°C. For bottom-up proteomics, dried venoms were reconstituted in buffer, reduced, alkylated, and trypsin-digested before HPLC-ESI-MS/MS analysis. HPLC-ESI-MS/MS analysis of ant venoms was carried out using Q Exactive Plus, Q Exactive HF, and Orbitrap Exploris hybrid quadrupole-orbitrap mass spectrometers equipped with ESI sources (Thermo Fisher Scientific) coupled to Dionex UltiMate or Vanquish Flex HPLC systems (Thermo Fisher Scientific). MALDI mass spectra were obtained with an Ultraflex III MALDI-TOF/TOF mass spectrometer (Bruker Daltonik, Bremen), operated in positive ionization and reflectron mode. For each measurement, 1000 spectra with a range of 600 to 5000 Da were accumulated. RNA was isolated from venom apparatuses (reservoir, duct, convoluted gland, and glandular filaments) and carcasses of at least 15 workers per colony using TRIzol extraction and sequenced to approximately 100,000,000 reads per sample on the Illumina HiSeq platform after poly(A) selection. Raw reads were quality-filtered using fastp and assembled using Trinity (*63*, *64*). For cross-species differential gene expression (DGE) analysis, a consensus genome and annotation were iteratively generated per sample to reduce reference bias, using trimmed and filtered RNA-seq reads mapped to the *C. floridanus* reference genome. Transcripts with high coverage were retained to define a baseline gene set. Expression differences were quantified using Bowtie2 (*65*), RSEM (*66*), and DESeq2 (*67*) following count aggregation with tximport (*68*). FRTX peptides were identified using BLAST (*69*) to search de novo sequences obtained from fragment ion mass spectra against transcriptome assemblies and confirmed by manual analysis of raw LC-MS data (top-down approach). Proteins were identified by matching MS raw data against transcriptome-derived protein databases and annotated using the *C. floridanus* RefSeq genome as a reference (bottom-up approach). Folded peptide structures were predicted using PepFold4 (all peptides) and AlphaFold3 ($FRTX_2$-Cflo1a) (*70*, *71*). Venom peptides were quantified against synthetic standards using HPLC-MS. Synthetic formicitoxins were prepared using microwave-assisted solid-phase peptide synthesis (Fmoc strategy), purified using reversed-phase HPLC, converted to their hydrochloride salts by repeated lyophilization from diluted hydrochloric acid, and used in experiments as dimethyl sulfoxide (DMSO) stock solutions. Insecticidal/insect paralyzing activities of formicitoxins and NAEs were determined by injection into *L. caesar* larvae at doses of 400 and 200 nmol, respectively. To determine the antibacterial effects of synthetic formicitoxins and NAEs, dilution series of compounds were prepared in MH-I medium, inoculated with bacteria, and growth curves were recorded using the optical density of the bacterial suspension at 600 nm. Hemolytic activity of the tested compounds was determined against sheep erythrocytes at 37°C for 1 hour in citric acid/phosphate buffers. *P. brocae* was isolated from an ant pupa covered in fungal spores, which originated from a lab-reared *C. nicobarensis* colony. This isolate was identified using DNA barcoding of the internal transcribed spacer (ITS) region of the rRNA cluster. The antifungal activities of formicitoxins and NAEs were assessed in a WST-8–based microtiter plate assay (*72*), in which dilution series of the test compounds in RPMI 1640 were inoculated with conidiospores and incubated for 2 days at 27°C in the presence of menadione and WST-8. Fungal growth was then quantified by photometric readout at 460 nm. For in vivo pupae infection experiments, *C. nicobarensis* pupae were treated with 3×10^5 *M. pingshaense* conidiospores and 96 pmol $FRTX_1$-Cnic1a or control solutions, placed in petri dishes in groups of four, and inspected daily for fungal outgrowth. Before AFM, fluorescence microscopy, and phase-contrast microscopy, conidiospores of *M. pingshaense* were diluted in phosphate-buffered saline (pH 7), test compounds were added as DMSO stocks, and spore suspensions were incubated for 18 hours at 27°C. Insertion of peptides from a phosphate buffer subphase into POPC monolayers was studied using film balance measurements and IRRAS. Orientations of the peptides in POPC monolayers were determined from angle- and polarization-dependent IRRAS experiments. A complete description of the materials and methods used in this study is provided in the Supplementary Materials.

Supplementary Materials

The PDF file includes:

Supplementary Materials and Methods
Supplementary Text
Figs. S1 to S79
Tables S1 to S5
Legends for data S1 to S17
References

Other Supplementary Material for this manuscript includes the following:

Data S1 to S17

REFERENCES

1. J. Wray, Extract of a letter, written by Mr. John Wray to the publisher January 13. 1670. Concerning some un-common observations and experiments made with an acid juyce to be found in ants. *Philos. Trans. R. Soc.* **5**, 2063–2066 (1670).

Downloaded from https://www.science.org at Cambridge University on July 16, 2026

2. F. Flury, Über die Bedeutung der Ameisensäure als natürlich vorkommendes Gift. *Ber. Dtsch. Pharm. Ges.* **29**, 650–669 (1919).
3. L. Koch, T. H. J. Niedermeyer, S. Tragust, Acid reign: Formicine ants and their venoms. *Myrmecol. News* **35**, 1–27 (2025).
4. V. Schendel, L. D. Rash, R. A. Jenner, E. A. B. Undheim, The diversity of venom: The importance of behavior and venom system morphology in understanding its ecology and evolution. *Toxins* **11**, 666 (2019).
5. O. Otti, S. Tragust, H. Feldhaar, Unifying external and internal immune defences. *Trends Ecol. Evol.* **29**, 625–634 (2014).
6. S. Tragust, External immune defence in ant societies (Hymenoptera: Formicidae): The role of antimicrobial venom and metapleural gland secretion. *Myrmecol. News* **23**, 119–128 (2016).
7. S. Tragust, C. Herrmann, J. Häfner, R. Braasch, C. Tilgen, M. Hoock, M. A. Milidakis, R. Gross, H. Feldhaar, Formicine ants swallow their highly acidic poison for gut microbial selection and control. *eLife* **9**, e60287 (2020).
8. H. R. Hermann, M. S. Blum, The hymenopterous poison apparatus. VI. *Camponotus pennsylvanicus* (Hymenoptera: Formicidae). *Psyche* **75**, 216–227 (1968).
9. M. F. H. Osman, J. Brander, Weitere Beiträge zur Kenntnis der chemischen Zusammensetzung des Giftes von Ameisen aus der Gattung *Formica*. *Z. Naturforsch. B* **16**, 749–753 (1961).
10. L. Kuhn-Nentwig, Antimicrobial and cytolytic peptides of venomous arthropods. *Cell. Mol. Life Sci.* **60**, 2651–2668 (2003).
11. S. J. M. Moreau, "It stings a bit but it cleans well": Venoms of Hymenoptera and their antimicrobial potential. *J. Insect Physiol.* **59**, 186–204 (2013).
12. S. Zheng, A. A. Doucette, Preventing *N*- and *O*-formylation of proteins when incubated in concentrated formic acid. *Proteomics* **16**, 1059–1068 (2016).
13. J. Lenčo, M. A. Khalikova, F. Švec, Dissolving peptides in 0.1% formic acid brings risk of artificial formylation. *J. Proteome Res.* **19**, 993–999 (2020).
14. A. Touchard, M. Dauvois, M.-J. Arguel, F. Petitclerc, M. Leblanc, A. Dejean, J. Orivel, G. M. Nicholson, P. Escoubas, Elucidation of the unexplored biodiversity of ant venom peptidomes via MALDI–TOF mass spectrometry and its application for chemotaxonomy. *J. Proteomics* **105**, 217–231 (2014).
15. B. Inceoglu, J. Lango, J. Jing, L. Chen, F. Doymaz, I. N. Pessah, B. D. Hammock, One scorpion, two venoms: Prevenom of *Parabuthus transvaalicus* acts as an alternative type of venom with distinct mechanism of action. *Proc. Natl. Acad. Sci. U.S.A.* **100**, 922–927 (2003).
16. E. D. Mock, B. Gagestein, M. van der Stelt, Anandamide and other *N*-acylethanolamines: A class of signaling lipids with therapeutic opportunities. *Prog. Lipid Res.* **89**, 101194 (2023).
17. N. Fornelos, E. A. Franzosa, J. Bishai, J. W. Annand, A. Oka, J. Lloyd-Price, T. D. Arthur, A. Garner, J. Avila-Pacheco, H. J. Haiser, A. C. Tolonen, J. A. Porter, C. B. Clish, R. B. Sartor, C. Huttenhower, H. Vlamakis, R. J. Xavier, Growth effects of *N*-acylethanolamines on gut bacteria reflect altered bacterial abundances in inflammatory bowel disease. *Nat. Microbiol.* **5**, 486–497 (2020).
18. L. Silva-Cardoso, P. Caccin, A. Magnabosco, M. Patrón, M. Targino, A. Fuly, G. A. Oliveira, M. H. Pereira, M. d. G. T. do Carmo, A. S. Souza, M. A. C. Silva-Neto, C. Montecucco, G. C. Atella, Paralytic activity of lysophosphatidylcholine from saliva of the waterbug *Belostoma anurum*. *J. Exp. Biol.* **213**, 3305–3310 (2010).
19. T. Jakob, M. M. Rauber, A. Perez-Riverol, E. Spillner, S. Blank, The honeybee venom major allergen Api m 10 (Icarapin) and its role in diagnostics and treatment of hymenoptera venom allergy. *Curr. Allergy Asthma Rep.* **20**, 48 (2020).
20. A. Touchard, V. Barassé, J.-M. Malgouyre, M. Treilhou, C. Klopp, E. Bonnafé, The genome of the ant *Tetramorium bicarinatum* reveals a tandem organization of venom peptides genes allowing the prediction of their regulatory and evolutionary profiles. *BMC Genomics* **25**, 84 (2024).
21. A. Isaksen, P. G. Nachtigall, R. A. Araya, J. H. Beh, S. D. Robinson, T. F. Hansen, E. A. B. Undheim, Genome of the green-head ant, *Rhytidoponera metallica*, reveals mechanisms of toxin evolution in a genetically hyper-diverse eusocial species. *Genome Biol.* **26**, 306 (2025).
22. S. D. Robinson, V. Schendel, C. I. Schroeder, S. Moen, A. Mueller, A. A. Walker, N. McKinnon, G. G. Neely, I. Vetter, G. F. King, E. A. B. Undheim, Intra-colony venom diversity contributes to maintaining eusociality in a cooperatively breeding ant. *BMC Biol.* **21**, 5 (2023).
23. J. Orivel, V. Redeker, J.-P. Le Caer, F. Krier, A.-M. Revol-Junelles, A. Longeon, A. Chaffotte, A. Dejean, J. Rossier, Ponericins, new antibacterial and insecticidal peptides from the venom of the ant *Pachycondyla goeldii*. *J. Biol. Chem.* **276**, 17823–17829 (2001).
24. R. Stumper, Das Gift der Ameisen. *Nat. Tech. Schweiz. Z. Naturwissenschaften* **4**, 295–299 (1923).
25. M. Hejníková, A. Tomčala, J. Černý, D. Kodrík, Melittin-The principal toxin of honeybee venom-Is also produced in the honeybee fat body. *Comp. Biochem. Physiol. Part B Comp. Biochem.* **281**, 109928 (2024).
26. A. Hefetz, M. S. Blum, Biosynthesis and accumulation of formic acid in the poison gland of the carpenter ant *Camponotus pennsylvanicus*. *Science* **201**, 454–455 (1978).
27. A. Hefetz, M. S. Blum, Biosynthesis of formic acid by the poison glands of formicine ants. *Biochim. Biophys. Acta Gen. Subj.* **543**, 484–496 (1978).
28. G. Kreil, L. Haiml, G. Suchanek, Stepwise cleavage of the pro part of promelittin by dipeptidylpeptidase IV. Evidence for a new type of precursor-product conversion. *Eur. J. Biochem.* **111**, 49–58 (1980).
29. N. G. Seidah, A. Prat, The biology and therapeutic targeting of the proprotein convertases. *Nat. Rev. Drug Discov.* **11**, 367–383 (2012).
30. S. A. Kozlov, E. V. Grishin, The universal algorithm of maturation for secretory and excretory protein precursors. *Toxicon* **49**, 721–726 (2007).
31. S. A. Nixon, S. D. Robinson, A. J. Agwa, A. A. Walker, S. Choudhary, A. Touchard, E. A. Undheim, A. Robertson, I. Vetter, C. I. Schroeder, A. C. Kotze, V. Herzig, G. F. King, Multipurpose peptides: The venoms of Amazonian stinging ants contain anthelmintic ponericins with diverse predatory and defensive activities. *Biochem. Pharmacol.* **192**, 114693 (2021).
32. S. D. Robinson, L. Kambanis, D. Clayton, H. Hinneburg, L. Corcilius, A. Mueller, A. A. Walker, A. Keramidas, S. S. Kulkarni, A. Jones, I. Vetter, M. Thaysen-Andersen, R. J. Payne, G. F. King, E. A. Undheim, A pain-causing and paralytic ant venom glycopeptide. *iScience* **24**, 103175 (2021).
33. A. Touchard, S. R. Aili, N. Téné, V. Barassé, C. Klopp, A. Dejean, R. M. Kini, L. C. Mrinalini, T. Jouenne, B. Lefranc, J. Leprince, P. Escoubas, G. M. Nicholson, M. Treilhou, E. Bonnafé, Venom peptide repertoire of the european myrmicine ant *Manica rubida*: Identification of insecticidal toxins. *J. Proteome Res.* **19**, 1800–1811 (2020).
34. J. Heep, A. Klaus, T. Kessel, M. Seip, A. Vilcinskas, M. Skaljac, Proteomic analysis of the venom from the ruby ant *Myrmica rubra* and the isolation of a novel insecticidal decapeptide. *Insects* **10**, 42 (2019).
35. S. D. Robinson, A. Mueller, D. Clayton, H. Starobova, B. R. Hamilton, R. J. Payne, I. Vetter, G. F. King, E. A. B. Undheim, A comprehensive portrait of the venom of the giant red bull ant, *Myrmecia gulosa*, reveals a hyperdiverse hymenopteran toxin gene family. *Sci. Adv.* **4**, eaau4640 (2018).
36. A. Rifflet, S. Gavalda, N. Téné, J. Orivel, J. Leprince, L. Guilhaudis, E. Génin, A. Vétillard, M. Treilhou, Identification and characterization of a novel antimicrobial peptide from the venom of the ant *Tetramorium bicarinatum*. *Peptides* **38**, 363–370 (2012).
37. N. Téné, E. Bonnafé, F. Berger, A. Rifflet, L. Guilhaudis, I. Ségalas-Milazzo, B. Pipy, A. Coste, J. Leprince, M. Treilhou, Biochemical and biophysical combined study of bicarinalin, an ant venom antimicrobial peptide. *Peptides* **79**, 103–113 (2016).
38. A. Touchard, S. R. Aili, E. G. P. Fox, P. Escoubas, J. Orivel, G. M. Nicholson, A. Dejean, The biochemical toxin arsenal from ant venoms. *Toxins* **8**, 30 (2016).
39. S. R. Aili, A. Touchard, P. Escoubas, M. P. Padula, J. Orivel, A. Dejean, G. M. Nicholson, Diversity of peptide toxins from stinging ant venoms. *Toxicon* **92**, 166–178 (2014).
40. D. Baracchi, S. Francese, S. Turillazzi, Beyond the antipredatory defence: Honey bee venom function as a component of social immunity. *Toxicon* **58**, 550–557 (2011).
41. D. Baracchi, S. Turillazzi, Differences in venom and cuticular peptides in individuals of *Apis mellifera* (Hymenoptera: Apidae) determined by MALDI-TOF MS. *J. Insect Physiol.* **56**, 366–375 (2010).
42. S. Turillazzi, G. Mastrobuoni, F. R. Dani, G. Moneti, G. Pieraccini, G. La Marca, G. Bartolucci, B. Perito, D. Lambardi, V. Cavallini, L. Dapporto, Dominulin A and B: Two new antibacterial peptides identified on the cuticle and in the venom of the social paper wasp *Polistes dominulus* Using MALDI-TOF, MALDI-TOF/TOF, and ESI-ion trap. *J. Am. Soc. Mass Spectrom.* **17**, 376–383 (2006).
43. M. S. Obin, R. K. V. Meer, Gaster flagging by fire ants (*Solenopsis* spp.): Functional significance of venom dispersal behavior. *J. Chem. Ecol.* **11**, 1757–1768 (1985).
44. M. Pusceddu, S. Tragust, P. Theodorou, I. C. Bolla, J. S. Navarro, F. Corrias, A. Atzei, A. Angioni, I. Floris, A. Satta, Varroa destructor weakens honey bee external immunity by impairing melittin production. *Sci. Rep.* **15**, 30623 (2025).
45. C. Tranter, P. Graystock, C. Shaw, J. F. S. Lopes, W. O. H. Hughes, Sanitizing the fortress: Protection of ant brood and nest material by worker antibiotics. *Behav. Ecol. Sociobiol.* **68**, 499–507 (2014).
46. S. Tragust, B. Mitteregger, V. Barone, M. Konrad, L. V. Ugelvig, S. Cremer, Ants disinfect fungus-exposed brood by oral uptake and spread of their poison. *Curr. Biol.* **23**, 76–82 (2013).
47. F. Bizzell, C. D. Pull, Ant queens cannibalise infected brood to contain disease spread and recycle nutrients. *Curr. Biol.* **34**, R848–R849 (2024).
48. C. D. Pull, L. V. Ugelvig, F. Wiesenhofer, A. V. Grasse, S. Tragust, T. Schmitt, M. J. F. Brown, S. Cremer, D. Tautz, Destructive disinfection of infected brood prevents systemic disease spread in ant colonies. *eLife* **7**, e32073 (2018).
49. S. Sauerländer, Das Gift von *Formica polyctena* Först. als ein möglicher Schutzmechanismus dieses Insekts gegen Mikroorganismen. *Naturwissenschaften* **48**, 629 (1961).
50. N. G. Oliveira Júnior, C. M. Souza, D. F. Buccini, M. H. Cardoso, O. L. Franco, Antimicrobial peptides: Structure, functions and translational applications. *Nat. Rev. Microbiol.* **23**, 687–700 (2025).
51. S. R. Dennison, F. Harris, M. Mura, D. A. Phoenix, An atlas of anionic antimicrobial peptides from amphibians. *Curr. Protein Pept. Sci.* **19**, 823–838 (2018).

Downloaded from https://www.science.org at Cambridge University on July 16, 2026

52. F. Harris, S. R. Dennison, D. A. Phoenix, Anionic antimicrobial peptides from eukaryotic organisms. *Curr. Protein Pept. Sci.* **10**, 585–606 (2009).
53. B. Schittek, R. Hipfel, B. Sauer, J. Bauer, H. Kalbacher, S. Stevanovic, M. Schirle, K. Schroeder, N. Blin, F. Meier, G. Rassner, C. Garbe, Dermcidin: A novel human antibiotic peptide secreted by sweat glands. *Nat. Immunol.* **2**, 1133–1137 (2001).
54. S. Ascoët, A. Touchard, N. Téné, B. Lefranc, J. Leprince, F. Paquet, L. Jouvensal, V. Barassé, M. Treilhou, A. Billet, E. Bonnafé, The mechanism underlying toxicity of a venom peptide against insects reveals how ants are master at disrupting membranes. *iScience* **26**, 106157 (2023).
55. S. A. Nixon, Z. Dekan, S. D. Robinson, S. Guo, I. Vetter, A. C. Kotze, P. F. Alewood, G. F. King, V. Herzig, It takes two: Dimerization is essential for the broad-spectrum predatory and defensive activities of the venom peptide Mp1a from the jack jumper ant *Myrmecia pilosula*. *Biomedicine* **8**, 185 (2020).
56. M. Schubert, D. Labudde, H. Oschkinat, P. Schmieder, A software tool for the prediction of Xaa-Pro peptide bond conformations in proteins based on ^{13}C chemical shift statistics. *J. Biomol. NMR* **24**, 149–154 (2002).
57. P. Calvez, É. Demers, É. Boisselier, C. Salesse, Analysis of the contribution of saturated and polyunsaturated phospholipid monolayers to the binding of proteins. *Langmuir* **27**, 1373–1379 (2011).
58. A. Blume, A comparative study of the phase transitions of phospholipid bilayers and monolayers. *Biochim. Biophys. Acta* **557**, 32–44 (1979).
59. C. E. Dempsey, The actions of melittin on membranes. *Biochim. Biophys. Acta Rev. Biomembr.* **1031**, 143–161 (1990).
60. M. Frick, C. Schwieger, C. Schmidt, Liposomes as carriers of membrane-associated proteins and peptides for mass spectrometric analysis. *Angew. Chem. Int. Ed.* **60**, 11523–11530 (2021).
61. E. Habermann, "Chemistry, pharmacology, and toxicology of bee, wasp, and hornet" in *Venomous Animals and Their Venoms*, W. Bücherl, E. E. Buckley, Eds. (Academic Press, 1971), pp. 61–93.
62. D. Dylus, A. Altenhoff, S. Majidian, F. J. Sedlazeck, C. Dessimoz, Inference of phylogenetic trees directly from raw sequencing reads using Read2Tree. *Nat. Biotechnol.* **42**, 139–147 (2024).
63. M. G. Grabherr, B. J. Haas, M. Yassour, J. Z. Levin, D. A. Thompson, I. Amit, X. Adiconis, L. Fan, R. Raychowdhury, Q. Zeng, Z. Chen, E. Mauceli, N. Hacohen, A. Gnirke, N. Rhind, F. Di Palma, B. W. Birren, C. Nusbaum, K. Lindblad-Toh, N. Friedman, A. Regev, Full-length transcriptome assembly from RNA-Seq data without a reference genome. *Nat. Biotechnol.* **29**, 644–652 (2011).
64. S. Chen, Y. Zhou, Y. Chen, J. Gu, fastp: An ultra-fast all-in-one FASTQ preprocessor. *Bioinf. (Oxf.)* **34**, i884–i890 (2018).
65. B. Langmead, S. L. Salzberg, Fast gapped-read alignment with Bowtie 2. *Nat. Methods* **9**, 357–359 (2012).
66. B. Li, C. N. Dewey, RSEM: Accurate transcript quantification from RNA-Seq data with or without a reference genome. *BMC Bioinformatics* **12**, 323 (2011).
67. M. I. Love, W. Huber, S. Anders, Moderated estimation of fold change and dispersion for RNA-seq data with DESeq2. *Genome Biol.* **15**, 550 (2014).
68. C. Soneson, M. I. Love, M. D. Robinson, Differential analyses for RNA-seq: Transcript-level estimates improve gene-level inferences. *F1000Res.* **4**, 1521 (2015).
69. C. Camacho, G. Coulouris, V. Avagyan, N. Ma, J. Papadopoulos, K. Bealer, T. L. Madden, BLAST+: Architecture and applications. *BMC Bioinformatics* **10**, 421 (2009).
70. J. Rey, S. Murail, S. de Vries, P. Derreumaux, P. Tuffery, PEP-FOLD4: A pH-dependent force field for peptide structure prediction in aqueous solution. *Nucleic Acids Res.* **51**, W432–W437 (2023).
71. J. Abramson, J. Adler, J. Dunger, R. Evans, T. Green, A. Pritzel, O. Ronneberger, L. Willmore, A. J. Ballard, J. Bambrick, S. W. Bodenstein, D. A. Evans, C.-C. Hung, M. O'Neill, D. Reiman, K. Tunyasuvunakool, Z. Wu, A. Žemgulytė, E. Arvaniti, C. Beattie, O. Bertolli, A. Bridgland, A. Cherepanov, M. Congreve, A. I. Cowen-Rivers, A. Cowie, M. Figurnov, F. B. Fuchs, H. Gladman, R. Jain, Y. A. Khan, C. M. R. Low, K. Perlin, A. Potapenko, P. Savy, S. Singh, A. Stecula, A. Thillaisundaram, C. Tong, S. Yakneen, E. D. Zhong, M. Zielinski, A. Žídek, V. Bapst, P. Kohli, M. Jaderberg, D. Hassabis, J. M. Jumper, Accurate structure prediction of biomolecular interactions with AlphaFold 3. *Nature* **630**, 493–500 (2024).
72. T. Tsukatani, H. Suenaga, M. Shiga, K. Matsumoto, A rapid microplate method for the proliferation assay of fungi and the antifungal susceptibility testing using the colorimetric microbial viability assay. *Lett. Appl. Microbiol.* **59**, 184–192 (2014).
73. J. Buellesbach, J. Rinke, L. Reuter, J. M. Thomas, V. Hartmann, M. Pohl, J. Gadau, U. R. Ernst, Conserved worker policing in African carpenter ants with drastically different egg chemotypes. *Evol. Ecol.* **37**, 815–834 (2023).
74. M. G. Murray, W. F. Thompson, Rapid isolation of high molecular weight plant DNA. *Nucleic Acids Res.* **8**, 4321–4326 (1980).
75. O. Folmer, M. Black, W. Hoeh, R. Lutz, R. Vrijenhoek, DNA primers for amplification of mitochondrial cytochrome c oxidase subunit I from diverse metazoan invertebrates. *Mol. Mar. Biol. Biotechnol.* **3**, 294–299 (1994).
76. T. J. White, T. Bruns, S. Lee, J. Taylor, "Amplification and direct sequencing of fungal ribosomal RNA genes for phylogenetics" in *PCR Protocols: A Guide to Methods and Applications*, M. A. Innis, D. H. Gelfand, J. J. Sninsky, T. J. White, Eds. (Academic Press, San Diego, 1990), pp. 315–322.
77. M. Gardes, T. D. Bruns, ITS primers with enhanced specificity for basidiomycetes-application to the identification of mycorrhizae and rusts. *Mol. Ecol.* **2**, 113–118 (1993).
78. B. Ma, K. Zhang, C. Hendrie, C. Liang, M. Li, A. Doherty-Kirby, G. Lajoie, PEAKS: Powerful software for peptide de novo sequencing by tandem mass spectrometry. *Rapid Commun. Mass Spectrom.* **17**, 2337–2342 (2003).
79. J. Morales-Sanfrutos, A. Megia-Fernandez, F. Hernandez-Mateo, M. D. Giron-Gonzalez, R. Salto-Gonzalez, F. Santoyo-Gonzalez, Alkyl sulfonyl derivatized PAMAM-G2 dendrimers as nonviral gene delivery vectors with improved transfection efficiencies. *Org. Biomol. Chem.* **9**, 851–864 (2011).
80. D. Gilbert, Gene-omes built from mRNA seq not genome DNA. *F1000Res.* **5**, 1695 (2016).
81. C. P. Cantalapiedra, A. Hernández-Plaza, I. Letunic, P. Bork, J. Huerta-Cepas, eggNOG-mapper v2: Functional annotation, orthology assignments, and domain prediction at the metagenomic scale. *Mol. Biol. Evol.* **38**, 5825–5829 (2021).
82. A. Astashyn, E. S. Tvedte, D. Sweeney, V. Sapojnikov, N. Bouk, V. Joukov, E. Mozes, P. K. Strope, P. M. Sylla, L. Wagner, S. L. Bidwell, L. C. Brown, K. Clark, E. W. Davis, B. Smith-White, W. Hlavina, K. D. Pruitt, V. A. Schneider, T. D. Murphy, Rapid and sensitive detection of genome contamination at scale with FCS-GX. *Genome Biol.* **25**, 60 (2024).
83. D. Blankenberg, G. von Kuster, E. Bouvier, D. Baker, E. Afgan, N. Stoler, J. Taylor, A. Nekrutenko, Galaxy team, dissemination of scientific software with galaxy ToolShed. *Genome Biol.* **15**, 403 (2014).
84. A. M. Altenhoff, A. Warwick Vesztrocy, C. Bernard, C.-M. Train, A. Nicheperovich, S. Prieto Baños, I. Julca, D. Moi, Y. Nevers, S. Majidian, C. Dessimoz, N. M. Glover, OMA orthology in 2024: Improved prokaryote coverage, ancestral and extant GO enrichment, a revamped synteny viewer and more in the OMA Ecosystem. *Nucleic Acids Res.* **52**, D513–D521 (2024).
85. M. Martin, Cutadapt removes adapter sequences from high-throughput sequencing reads. *EMBnet.J* **17**, 10–12 (2011).
86. Z.-L. Deng, P. C. Münch, R. Mreches, A. C. McHardy, Rapid and accurate identification of ribosomal RNA sequences via deep learning. *Nucleic Acids Res.* **50**, e60 (2022).
87. A. Dobin, C. A. Davis, F. Schlesinger, J. Drenkow, C. Zaleski, S. Jha, P. Batut, M. Chaisson, T. R. Gingeras, STAR: Ultrafast universal RNA-seq aligner. *Bioinformatics* **29**, 15–21 (2013).
88. P. Danecek, J. K. Bonfield, J. Liddle, J. Marshall, V. Ohan, M. O. Pollard, A. Whitwham, T. Keane, S. A. McCarthy, R. M. Davies, H. Li, Twelve years of SAMtools and BCFtools. *GigaScience* **10**, giab008 (2021).
89. A. S. Hinrichs, D. Karolchik, R. Baertsch, G. P. Barber, G. Bejerano, H. Clawson, M. Diekhans, T. S. Furey, R. A. Harte, F. Hsu, J. Hillman-Jackson, R. M. Kuhn, J. S. Pedersen, A. Pohl, B. J. Raney, K. R. Rosenbloom, A. Siepel, K. E. Smith, C. W. Sugnet, A. Sultan-Qurraie, D. J. Thomas, H. Trumbower, R. J. Weber, M. Weirauch, A. S. Zweig, D. Haussler, W. J. Kent, The UCSC genome browser database: Update 2006. *Nucleic Acids Res.* **34**, D590–D598 (2006).
90. K. Tamura, Estimation of the number of nucleotide substitutions when there are strong transition-transversion and G+C-content biases. *Mol. Biol. Evol.* **9**, 678–687 (1992).
91. K. Tamura, G. Stecher, S. Kumar, MEGA11: Molecular evolutionary genetics analysis version 11. *Mol. Biol. Evol.* **38**, 3022–3027 (2021).
92. I. Koludarov, M. Velasque, T. Senoner, T. Timm, C. Greve, A. B. Hamadou, D. K. Gupta, G. Lochnit, M. Heinzinger, A. Vilcinskas, R. Gloag, B. A. Harpur, L. Podsiadlowski, B. Rost, T. N. W. Jackson, S. Dutertre, E. Stolle, B. M. von Reumont, Prevalent bee venom genes evolved before the aculeate stinger and eusociality. *BMC Biol.* **21**, 229 (2023).
93. A. R. Quinlan, I. M. Hall, BEDTools: A flexible suite of utilities for comparing genomic features. *Bioinformatics* **26**, 841–842 (2010).
94. J. Trifinopoulos, L.-T. Nguyen, A. von Haeseler, B. Q. Minh, W-IQ-TREE: A fast online phylogenetic tool for maximum likelihood analysis. *Nucleic Acids Res.* **44**, W232–W235 (2016).
95. F. Teufel, J. J. Almagro Armenteros, A. R. Johansen, M. H. Gíslason, S. I. Pihl, K. D. Tsirigos, O. Winther, S. Brunak, G. von Heijne, H. Nielsen, SignalP 6.0 predicts all five types of signal peptides using protein language models. *Nat. Biotechnol.* **40**, 1023–1025 (2022).
96. W. O. H. Hughes, L. Thomsen, J. Eilenberg, J. J. Boomsma, Diversity of entomopathogenic fungi near leaf-cutting ant nests in a neotropical forest, with particular reference to *Metarhizium anisopliae* var. *anisopliae*. *J. Invertebr. Pathol.* **85**, 46–53 (2004).
97. C. D. Pull, W. O. H. Hughes, M. J. F. Brown, Tolerating an infection: An indirect benefit of co-founding queen associations in the ant *Lasius niger*. *Naturwissenschaften* **100**, 1125–1136 (2013).
98. D. T. Vistica, P. Skehan, D. Scudiero, A. Monks, A. Pittman, M. R. Boyd, Tetrazolium-based assays for cellular viability: A critical examination of selected parameters affecting formazan production. *Cancer Res.* **51**, 2515–2520 (1991).
99. P. Tufféry, P. Derreumaux, A refined pH-dependent coarse-grained model for peptide structure prediction in aqueous solution. *Front. Bioinform.* **3**, 1113928 (2023).
100. V. Binette, N. Mousseau, P. Tuffery, A generalized attraction-repulsion potential and revisited fragment library improves PEP-FOLD peptide structure prediction. *J. Chem. Theory Comput.* **18**, 2720–2736 (2022).

Downloaded from https://www.science.org at Cambridge University on July 16, 2026

101. M. R. Wilkins, E. Gasteiger, A. Bairoch, J. C. Sanchez, K. L. Williams, R. D. Appel, D. F. Hochstrasser, Protein identification and analysis tools in the ExPASy server. *Methods Mol. Biol.* **112**, 531–552 (1999).
102. R Development Core Team, *R: A Language and Environment for Statistical Computing* (R Foundation for Statistical Computing, 2020).
103. H. Wickham, J. Hester, R. François, readr: Read rectangular text data. R package version 2.1.5 (2018); https://github.com/tidyverse/readr.
104. H. Wickham, *ggplot2: Elegant Graphics for Data Analysis* (Springer-Verlag, 2016).
105. J. Schindelin, I. Arganda-Carreras, E. Frise, V. Kaynig, M. Longair, T. Pietzsch, S. Preibisch, C. Rueden, S. Saalfeld, B. Schmid, J.-Y. Tinevez, D. J. White, V. Hartenstein, K. Eliceiri, P. Tomancak, A. Cardona, Fiji: An open-source platform for biological-image analysis. *Nat. Methods* **9**, 676–682 (2012).
106. J. L. Markley, A. Bax, Y. Arata, C. W. Hilbers, R. Kaptein, B. D. Sykes, P. E. Wright, K. Wüthrich, Recommendations for the presentation of NMR structures of proteins and nucleic acids. *J. Mol. Biol.* **280**, 933–952 (1998).
107. J. C. Hoch, K. Baskaran, H. Burr, J. Chin, H. R. Eghbalnia, T. Fujiwara, M. R. Gryk, T. Iwata, C. Kojima, G. Kurisu, D. Maziuk, Y. Miyanoiri, J. R. Wedell, C. Wilburn, H. Yao, M. Yokochi, Biological magnetic resonance data bank. *Nucleic Acids Res.* **51**, D368–D376 (2023).
108. V. L. Kuz'min, Alexander V. Mikhailov, Molecular theory of light reflection and applicability limits of the macroscopic approach. *Opt. Spectrosc.* (1981).
109. V. L. Kuzmin, V. P. Romanov, A. V. Mikhailov, Reflection of light at the boundary of liquid systems and structure of the surface layer: A review. *Opt. Spectrosc.* **73**, 1–26 (1989).
110. C. Schwieger, B. Chen, C. Tschierske, J. Kressler, A. Blume, Organization of T-shaped facial amphiphiles at the air/water interface studied by infrared reflection absorption spectroscopy. *J. Phys. Chem. B* **116**, 12245–12256 (2012).
111. J. E. Bertie, M. K. Ahmed, H. H. Eysel, Infrared intensities of liquids. 5. Optical and dielectric constants, integrated intensities, and dipole moment derivatives of H_2O and D_2O at 22 °C. *J. Phys. Chem.* **93**, 2210–2218 (1989).
112. J. E. Bertie, Z. Lan, Infrared intensities of liquids XX: The intensity of the OH stretching band of liquid water revisited, and the best current values of the optical constants of H_20(l) at 25 °C between 15,000 and 1 cm^{-1}. *Appl. Spectrosc.* **50**, 1047–1057 (1996).
113. G. F. King, M. C. Gentz, P. Escoubas, G. M. Nicholson, A rational nomenclature for naming peptide toxins from spiders and other venomous animals. *Toxicon* **52**, 264–276 (2008).
114. E. A. Undheim, A. Jones, K. R. Clauser, J. W. Holland, S. S. Pineda, G. F. King, B. G. Fry, Clawing through evolution: Toxin diversification and convergence in the ancient lineage chilopoda (Centipedes). *Mol. Biol. Evol.* **31**, 2124–2148 (2014).
115. S. B. Needleman, C. D. Wunsch, A general method applicable to the search for similarities in the amino acid sequence of two proteins. *J. Mol. Biol.* **48**, 443–453 (1970).
116. M. Wang, A. K. Jarmusch, F. Vargas, A. A. Aksenov, J. M. Gauglitz, K. Weldon, D. Petras, R. da Silva, R. Quinn, A. V. Melnik, J. J. J. van der Hooft, A. M. Caraballo-Rodríguez, L. F. Nothias, C. M. Aceves, M. Panitchpakdi, E. Brown, F. Di Ottavio, N. Sikora, E. O. Elijah, L. Labarta-Bajo, E. C. Gentry, S. Shalapour, K. E. Kyle, S. P. Puckett, J. D. Watrous, C. S. Carpenter, A. Bouslimani, M. Ernst, A. D. Swafford, E. I. Zúñiga, M. J. Balunas, J. L. Klassen, R. Loomba, R. Knight, N. Bandeira, P. C. Dorrestein, Mass spectrometry searches using MASST. *Nat. Biotechnol.* **38**, 23–26 (2020).
117. M. A. Hoffmann, L.-F. Nothias, M. Ludwig, M. Fleischauer, E. C. Gentry, M. Witting, P. C. Dorrestein, K. Dührkop, S. Böcker, High-confidence structural annotation of metabolites absent from spectral libraries. *Nat. Biotechnol.* **40**, 411–421 (2022).
118. S. Böcker, M. C. Letzel, Z. Lipták, A. Pervukhin, SIRIUS: Decomposing isotope patterns for metabolite identification. *Bioinformatics* **25**, 218–224 (2009).

Acknowledgments: We thank A. Schmidt and B. Barabás for bioinformatics prototyping during their BSc theses at the Institute of Computer Science; J. Gadau, E. Frank, and H. Feldhaar for providing *Camponotus* samples; C. Übensee for technical assistance with DNA extractions; and Z. Zhao for the photograph of *C. fellah*. We thank M. Fuszard and the core facility for proteomic mass spectrometry of the Martin Luther University Halle-Wittenberg for providing access to analysis software. **Funding:** This work was supported by grants from the German Research Foundation: DFG project 467315902 (E. Dittmann), DFG project INST 271/388-1 (T.H.J.N.), DFG project EXC2124 (H.B.-O. and E.L.), DFG project 520989725 (S.T.), and DFG project 570426511 (S.T.). We acknowledge the Core Facility BioSupraMol of the Freie Universität Berlin, supported by the DFG, for MS and NMR measurements. We acknowledge financial support within the funding program Open Access Publishing by the German Research Foundation (DFG). L. Koch received a state scholarship (Landesgraduiertenförderung) from MLU Halle-Wittenberg and the federal state of Saxony-Anhalt. pH measurements of pupae using a VisiSens optical pH sensing system were funded by a research grant from the Ethologische Gesellschaft e.V. (S.T.). **Author contributions:** Conceptualization: L. Koch, S.T., and T.H.J.N. Methodology: B.F., C.S., F.H., H.B.-O., L. Koch, M.H., M.M., S.A., S.T., and T.H.J.N. Investigation: A.M.Z., A.S., B.F., B.-F.H., E.L., J.G., L. Koch, L. Kolhoff, M.H., N.N.W., M. Schub., S.A., S.T., and V.I.C.R. Resources: A.C.L., A.S., M. Schut., N.N.W., and S.T. Visualization: L. Koch, M. Schub., and S.T. Funding acquisition: H.B.-O., L. Koch, S.T., and T.H.J.N. Project administration: L. Koch, S.T., and T.H.J.N. Supervision: H.B.-O., S.T., and T.H.J.N. Validation: S.A., S.T., and T.H.J.N. Data curation: M. Schub. and S.T. Formal analysis: B.F., M. Schub., S.A., and S.T. Writing—original draft: L. Koch, and M. Schub.. Writing—review and editing: A.C.L., A.S., B.F., C.S., E.L., F.H., H.B.-O., L. Koch, L. Kolhoff, M.H., M.M., M. Schub., N.N.W., S.A., S.T., T.H.J.N., and V.I.C.R. **Competing interests:** The authors declare that they have no competing interests. **Data, code, and materials availability:** HPLC-MS/MS data of *Camponotus* venoms are available as MassIVE datasets MSV000098463 (neat venoms, https://doi.org/doi:10.25345/C5J67988C) and MSV000099392 (reduced, carbamidomethylated, and trypsin-digested venoms, https://doi.org/doi:10.25345/C5HH6CK18). MALDI-MS data of *C. nicobarensis* venom can be accessed as MassIVE dataset MSV000099024 (https://doi.org/10.25345/C5FJ29R9R). MS spectra of synthetic and natural linoleoyl ethanolamide, oleoyl ethanolamide, linoleamidoethyl formate, and oleamidoethyl formate were deposited as MassIVE dataset MSV000098423 (https://doi.org/doi:10.25345/C5Q52FR93). Mitochondrial cytochrome c oxidase subunit I DNA barcoding sequences of *Camponotus* samples (GenBank accessions PX048962 to PX048978 at https://www.ncbi.nlm.nih.gov/genbank/), internally transcribed spacer region DNA barcoding sequences of fungal strains (GenBank accessions PX058095 to PX058097 at https://www.ncbi.nlm.nih.gov/genbank/), RNA-seq data of venom glands and carcasses, and transcriptome assemblies (TSA accessions GLJC00000000, GLJG00000000, GLJH00000000, GLJI00000000, GLJJ00000000, GLJK00000000, GLJL00000000, GLJM00000000, GLJN00000000, GLJO00000000, GLJP00000000, GLJR00000000, and GLJS00000000 at https://www.ncbi.nlm.nih.gov/genbank/tsa/), and sequences of mRNAs coding for FRTX peptides (GenBank accessions PX848779 to PX848826) can be accessed as NIH BioProject PRJNA1286179 (https://www.ncbi.nlm.nih.gov/bioproject/PRJNA1286179/). Annotated transcriptome assemblies are available at figshare (https://doi.org/10.6084/m9.figshare.30086413). NMR spectra of synthetic linoleoyl ethanolamide, oleoyl ethanolamide, linoleamidoethyl formate, and oleamidoethyl formate were deposited at nmrXive (https://doi.org/10.57992/NMRXIV.P118). NMR spectra of $FRTX_1$-Cnic1a and $FRTX_2$-Cflo1a can be accessed at the BioMagResBank as entries 53213 (https://doi.org/10.13018/BMR53213) and 53225 (https://doi.org/10.13018/BMR53225). This study did not generate new materials.

Submitted 27 October 2025
Accepted 10 April 2026
Published 13 May 2026
10.1126/sciadv.aed4078

Downloaded from https://www.science.org at Cambridge University on July 16, 2026

ScienceAdvances

Beyond formic acid: Peptides in carpenter ant venoms aid in disease protection

Lukas Koch, Sandro Andreotti, Mario Schubert, Elisa Liebhart, Anton M. Zürbig, Julian Gatzki, Benjamin-Florian Hempel, Lydia Kollhoff, Barbara Feldmeyer, Martin Herzberg, Valerie I. C. Rebhahn, Nwet Nwet Win, Adria C. LeBoeuf, Marat Meleshin, Fabian Herrmann, Christian Schwieger, Heike Brötz-Oesterhelt, Andrea Sinz, Mike Schutkowski, Timo H. J. Niedermeyer, and Simon Tragust

Sci. Adv. **12** (20), eaed4078. DOI: 10.1126/sciadv.aed4078

View the article online
https://www.science.org/doi/10.1126/sciadv.aed4078
Permissions
https://www.science.org/help/reprints-and-permissions

Downloaded from https://www.science.org at Cambridge University on July 16, 2026

Use of this article is subject to the Terms of service

Science Advances (ISSN 2375-2548) is published by the American Association for the Advancement of Science. 1200 New York Avenue NW, Washington, DC 20005. The title *Science Advances* is a registered trademark of AAAS.

Copyright © 2026 The Authors, some rights reserved; exclusive licensee American Association for the Advancement of Science. No claim to original U.S. Government Works. Distributed under a Creative Commons Attribution NonCommercial License 4.0 (CC BY-NC).